

MICROSTRUCTURE AND PREPARATION OF Ni, Al AND Fe NANOPOWDERS^①

Wei Qin^{a,b}, Lai Yingling^a, Yang Hong^a, Li Changgeng^a

*a Department of Applied Physics and Heat Engineering,
Central South University of Technology, Changsha 410083*

b International Centre for Materials Physics, Chinese Academy of Sciences, Shenyang 110015

ABSTRACT By means of mechanical-physical solid state reaction methods (MPSSRM), 5~25 nm powders of iron, nickel, aluminium have been prepared. The powders exhibit few clusters of monocrystal and polycrystal, the electronic structure of which were identified by X-ray diffraction and XPS. The experiments show that there is an oxide layer on the surfaces of Ni, Al, Fe nanopowders. DTA experiments show that the peak point temperature of primal temperature decreases with the decrease of the particle diameter, and tends to move in low temperature direction on the DTA curve of Fe nanopowder. The relationship between the particle diameter (d) of Fe nanopowder and surface energy (ΔH) can be given by $\Delta H \propto d^{-\frac{1}{2}}$.

Key words nanopowder microstructure electronic structure surface energy

1 INTRODUCTION

The nanopowder (5~100 nm) exhibits extraordinary properties of electricity, magnetism, mechanics and optics^[1]. The cost for Ni, Al, Fe nanopowders prepared by inert gas condensation method is very high. The preparation of *fcc* Al, Ni nanopowders by the ball milling method is difficult^[2]. By means of the mechanical-physical solid state reaction methods 5~25 nm Ni, Al, Fe powders have been successfully prepared in flowing Ar^[3]. The surface structure and surface compositions for Ni, Al, Fe nanopowders have been observed by TEM, XRD and XPS in this paper and the surface energy of Fe nanopowder is discussed.

2 EXPERIMENTAL METHOD

2.1 Sample preparation

The equipment of mechanical-physical solid state reaction methods (MPSSRM) was equipped with a planetary milling tool (rotation speed 250 r/min), a vacuum system and a pro-

TECTIVE atmosphere system in flowing Ar^[3]. The particle diameters of Ni, Al, Fe primal powders are about 44~17 μm . The nanopowders were treated 15, 20, 40, 60 and 82 h respectively in the equipment.

2.2 TEM, XRD, XPS and DTA experiments

The diameters of Ni, Al, Fe nanopowders were observed in a H-800 electron microscopy (using 75 kV, magnification 50 000~150 000 \times). The experiments of X-ray diffraction for Ni, Al, Fe nanopowders were measured with a D-500 X-ray diffractometer (using Ni filtered, Cu K_α radiation, 40 kV, 35 mA, scanning velocity 1.2°/min).

The XPS for Ni, Al, Fe nanopowders were recorded by means of ESCALAB-MK II electron spectrometer with base pressure of 7×10^{-8} Pa in the specimen preparation chamber and 5×10^{-8} Pa in the analysis chamber. The exciting source is Al K_α (1486.6 eV) radiation, 15 kV, 20 mA for XPS. The DTA experiment for Fe nanopowder were performed by means of a Dupont 9900 differential thermal analyser, from

① Received Mar. 11, 1996; accepted Jul. 24, 1996

room temperature to 750 °C, with Al_2O_3 crucible, at a temperature rising rate of 15 °C/min.

3 RESULTS AND DISCUSSION

3.1 Measurement of the particle diameter of Ni, Al, Fe nanopowders

Fig. 1 (a), (b), (c) show TEM images of Ni, Al, Fe nanopowders. The particle diameters of Ni, Al, Fe nanopowder were respectively 24, 10, 7 nm. Fig. 2 shows Fe nanopowder “crystal-



Fig. 1 TEM of Ni, Al, Fe nanopowders
(a) —Ni nanopowder(24 nm); (b) —Al nanopowder (10 nm); (c) —Fe nanopowder(7 nm)

line size—treated time”(15, 20, 40, 60, 82 h) curve. The nanopowder diameter decreases with the increase of treated time.

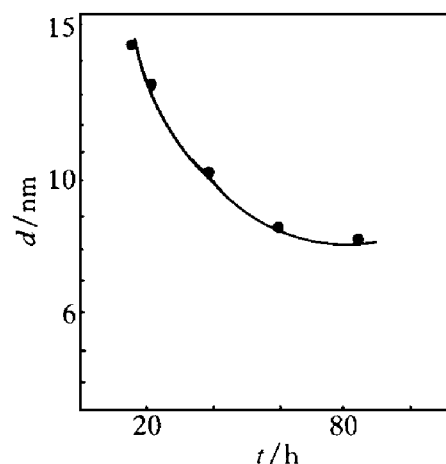


Fig. 2 “Crystalline size—treated time” curve of Fe nanopowders

3.2 Crystalline structure of Ni, Al, Fe nanopowder

Fig. 3 shows the electron diffraction patterns for Ni, Al, Fe nanopowder cluster. It is indicated that Ni, Al, Fe nanopowder is a cluster of the monocrystal and polycrystal.

The experiment shows that the equipment of MPSSRM can provide a complex force for metal powders during forming nanocrystalline grain, then the repeated impact tests extend to change the form of the metal crystal. This process is similar in some respects to modeling of hot isostatic pressing and superplastic forming, through which the crystal defect density increases. The fracture was intensified when crystal defect density realized a critical level. Therefore, it can be concluded that the nanopowder was formed by way of all complicated force at ambient temperature. There is difference on the electron diffraction patterns depending upon directionless of the nanocrystalline grain boundaries.

3.3 Phase analyses for Ni, Al, Fe nanopowders

Fig. 4 shows the X-ray diffractive patterns of Ni, Al, Fe nanopowders. It was indicated that Ni, Al, Fe nanopowders were *fcc* Ni, *fcc* Al and *bcc* α -Fe. There is no diffractive pattern of the metal oxide phase in Fig. 4.

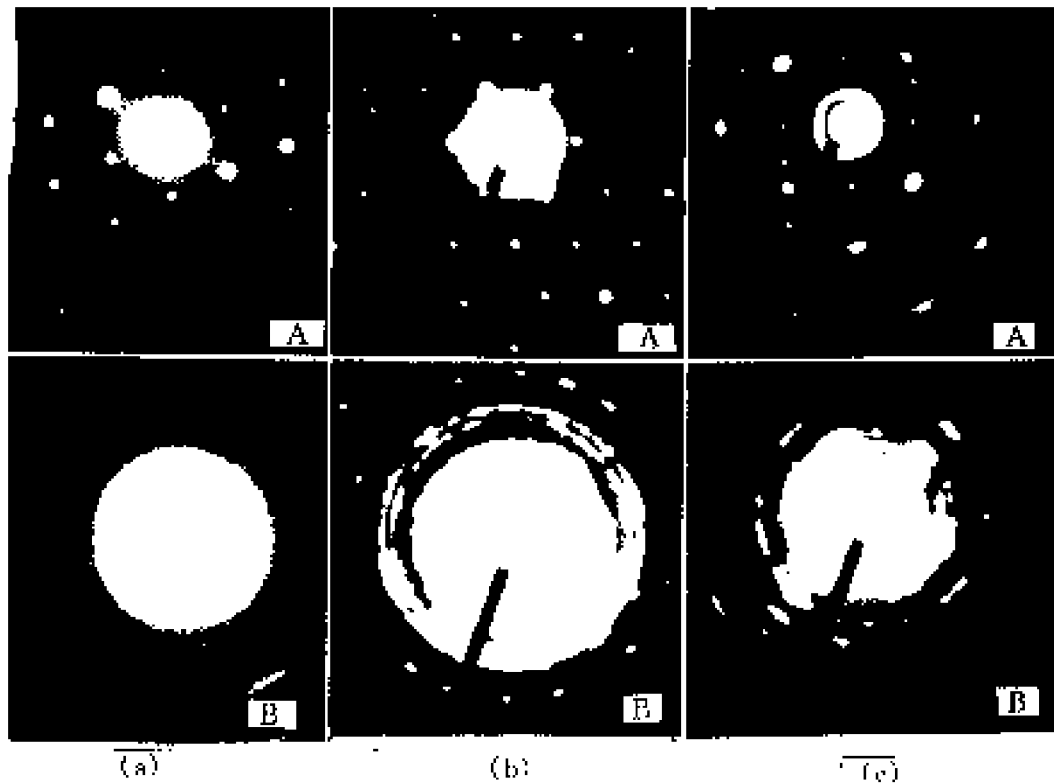


Fig. 3 Electron diffractive patterns of Ni, Al, Fe nanometer cluster

(a) —Ni (A— monocrystal, B— polycrystal); (b) —Al (A— monocrystal, B— polycrystal);
(c) —Fe (A— monocrystal, B— polycrystal)

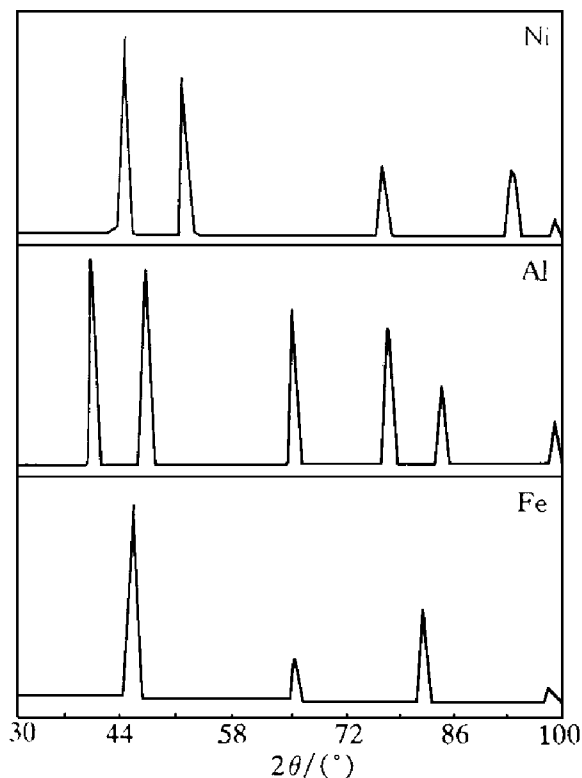


Fig. 4 XRD patterns of Ni, Al, Fe nanopowders

3. 4 Surface oxide layer and electronic structure of Ni, Al, Fe nanopowders

The phase analyses for Ni, Al, Fe nanopowders are shown by X-ray diffraction. The experiments indicate that the oxides compounds were not induced by MPSSRM. Fig. 5 shows XPS of Ni, Al, Fe nanopowder. There is a thin oxide layer on the surface of Ni primitive powder (Fig. 5 a₁, B), and Ni element peak was formed on the surface of Ni nanopowder during preparative process(Fig. 5 a₂, A).

There are oxide layer peak and Al element peak (Fig. 5 (b) b₁A, B) on the XPS of 16.8 μm Al powder. The Al element peak on XPS of Al nanopowder decreased with particle diameter to decrease. It was indicated that the surface of Al nanopowder is oxidated easily (Fig. 5 (b) b₂ A, B). The XPS of 10nm Fe nanopowder shows only Fe₂O₃ electron spectrum (Fig. 5 (c)). But Fe₂O₃ phase could not be found on X-ray diffraction pattern of Fe nanopowder, so that Fe₂O₃ layer was formed on the surface of Fe nanometer crystal. Tables 1, 2, 3 show the chemical shift of the core level for Ni, Al, Fe

atoms of the nanometer cluster. Tables 1, 2 show the level of the chemical shift for Ni, Al powders was changed with particle dimension. When 44 μm Ni powder has become 24 nm, ESCA shift of $\text{Ni}2P_{1/2}$ is “- 3.07 eV”. But 16.8 μm Al powder has become 15 nm, ESCA shift of $\text{Al}2P_{1/2}$ is “- 0.3 eV”. In the region of nanometer particle, the change of ESCA shift is more little, the 24 nm Ni powder has become 4.2 nm, ESCA shift of $\text{Ni}2P_{1/2}$ is “- 0.34 eV”, the 15 nm Al powder has become 11 nm, ESCA shift is “+ 0.1 eV”. Table 3 shows the chemical shift of Fe_2O_3 layer on the surface of Fe nanometer cluster differs from those on the surface of Ni nanometer cluster and Al nanometer cluster. The XPS of Fe element is not observed on the surface of Fe powder. The 44 μm Fe powder has become 10 nm, ESCA shift of $\text{Fe}2P_{1/2}$ of Fe_2O_3 layer is “- 0.1 eV”. The chemical shift of $\text{Fe}2P_{1/2}$ has not changed in the particle diameter from 10 to 7 nm. Tables 1, 2, 3 indicate that the change of the electronic structure of Ni, Al, Fe nanopowders is great during the process of forming nanopowder by MPSSRM. However the oxidizabilities of Ni, Al, Fe atoms are obvious different.

ous different.

3.5 Measurement of surface energy of Fe nanometer cluster

Fig. 6 (a), (b), (c) show DTA curve of Fe powder (particle diameter 44 μm , 10 nm, 7 nm). The preliminary transitional temperature on the DTA curve tends to become lower with the decrease of the particle diameter. Their preliminary temperatures are 435.52, 313.83 and 249.08 $^{\circ}\text{C}$, and the corresponding particle diameters are 44 μm , 10 nm, 7 nm respectively, these temperatures of peak point are 622.69, 503.64, 474.61 $^{\circ}\text{C}$.

Table 4 shows the results of the different

Table 1 Binding energies of $\text{Ni}2P_{3/2}$ and $\text{Ni}2P_{1/2}$ in different diameters

<i>d</i>	Ni $2P_{3/2}$		Ni $2P_{1/2}$	
	E_{B_1}	ΔE_{B_1}	E_{B_2}	ΔE_{B_2}
	/ eV	/ eV	/ eV	/ eV
44 μm	—	—	872.91	—
24 nm	852.50	—	869.84	- 3.07
4.2 nm	853.10	+ 0.60	869.50	- 0.34

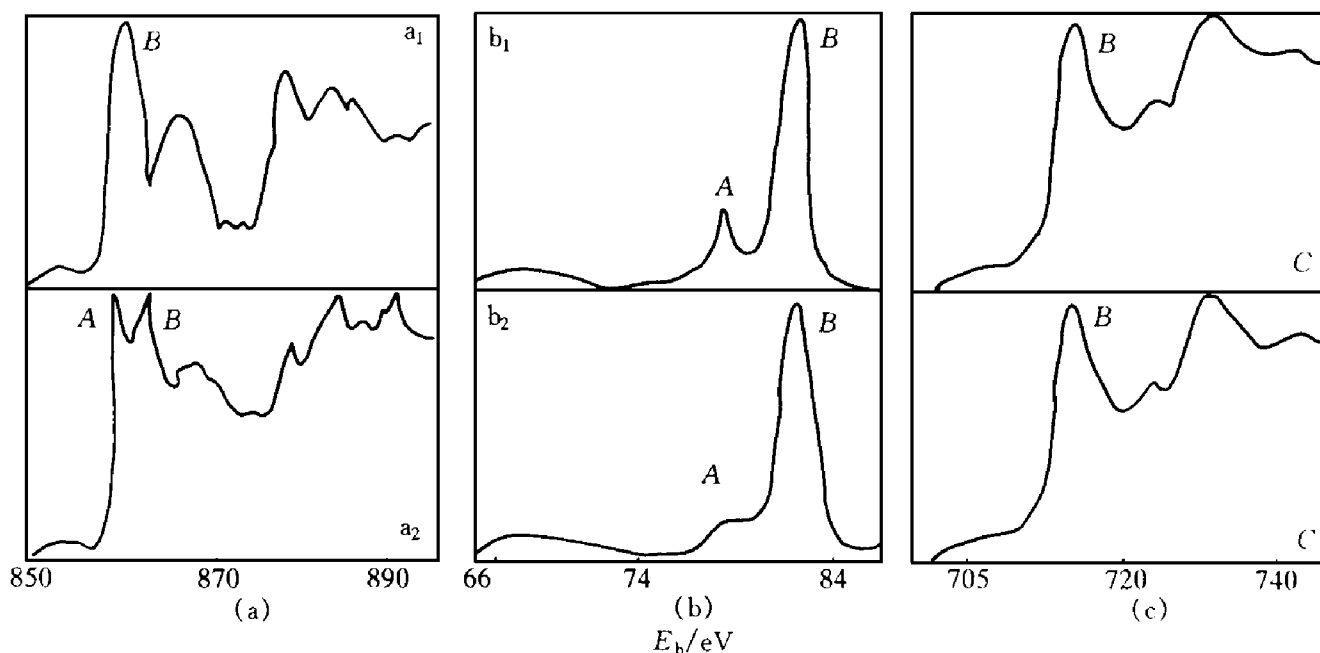


Fig. 5 XPS of Ni, Al, Fe nanopowders

a_1 —Ni powder (44 μm); a_2 —Ni nanopowder (24 nm) b_1 —Al powder (16.8 μm);

b_2 —Al nanopowder (11 nm); (c) — Fe_2O_3 of Fe powder or 10 nm Fe nanopowder;

A —element peak; B —oxide layer peak

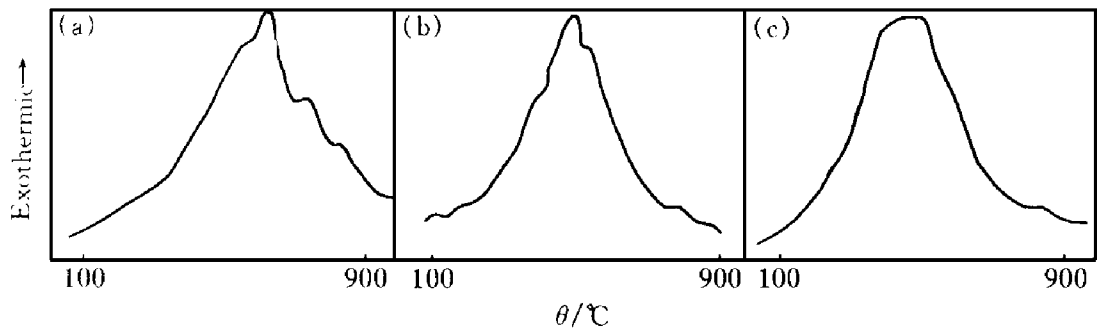


Fig. 6 DTA curve of Fe powder

(a) —particle diameter 44 μm; (b) —particle diameter 10 nm; (c) —particle diameter 7 nm

diameter particles measured by means of weighing method on the DTA area. The relation

tion between the surface energy (ΔH) and d is $\Delta H \propto d^{-1/2}$ for Fe nanometer cluster.

Table 2 Binding energies of $Al2P_{3/2}$ and $Al2P_{1/2}$ in different diameters

d	Al		$2P_{3/2}$		Al		$2P_{1/2}$	
	E_{B_1}		ΔE_{B_1}		E_{B_2}		ΔE_{B_2}	
	/ eV		/ eV		/ eV		/ eV	
16. 8μm	71. 20	—	—	—	74. 30	—	—	—
15nm	71. 00	—	0. 20	—	74. 00	—	0. 30	—
11nm	71. 10	—	0. 1	—	74. 10	—	0. 1	—

Table 3 Binding energies $Fe2P_{3/2}$ and $Fe2P_{1/2}$ in different diameters

d	$Fe2P_{3/2}$		$Fe2P_{1/2}$		$Fe2P_{3/2}$		$Fe2P_{1/2}$	
	E_{B_1}		ΔE_{B_1}		E_{B_2}		ΔE_{B_2}	
	/ eV		/ eV		/ eV		/ eV	
44μm	710. 80	—	—	—	724. 40	—	—	—
10nm	710. 70	—	0. 1	—	724. 30	—	0. 1	—
7nm	710. 70	—	0	—	724. 30	—	0	—

Table 4 DTA measures level

d	T_1 / °C	T_2 / °C	A / g	$d^{1/2}$	$\frac{A \bullet}{d^{1/2}}$
44μm	435. 52	622. 69	3. 3965	—	—
10nm	313. 83	503. 64	3. 0580	3. 26	9. 96
7nm	249. 03	474. 61	3. 8230	2. 63	10. 04

T_1 —preliminary transitional temperature;
 T_2 —park point temperature;
 A —peak area (weighing method g) .

between the peak area of the different particle diameter and $d^{1/2}$ (d —particle diameter) is obtained by counting method in Table 4. The rela-

4 CONCLUSIONS

- (1) The crystal structures of Ni, Al, Fe nanopowders are *fcc*, *bcc* and *fcc* respectively. The nanopowder is a mixture cluster of the monocrystal and polycrystal. There is an oxide layer (NiO, Al_2O_3 , Fe_2O_3) on the surface of the nanometer crystal(thickness 1~ 2 nm) .
- (2) The electronic structure between the large particle and nanometer particle for Ni, Al, Fe powders is different obviously. The changes of the electronic structure for Ni, Al, Fe nanopowders are different too, during the process of forming nanopowder by MPSSRM. However, the oxidizabilities of Ni, Al, Fe atom are obviously different.
- (3) The preliminary transitional temperature and peak point temperature tend to become lower with the decrease of the particle diameter on DTA curve of Fe nanopowder. The interface area of Fe nanopowder increases with the decrease of particle diameter. The relation between the surface energy (ΔH) and particle diameter (d) is $\Delta H \propto d^{-1/2}$.

REFERENCES

1 Kubo R. J Phys Soc of Japn, 1962, (17) : 975.
2 Brun L R *et al.* Metallurgica et Materialia, 1992, 26 (11): 1742.
3 Wei Qin *et al.* Journal of Central South Institute of Mining and Metallurgy(in Chinese), 1994, 25(1) : 137.
(Edited by Zhu Zhongguo)